^{13}C NMR Study of the Kinetics of the Functionalization of Poly(methyl acrylate) by Reaction with Ethanolamine

Youlu Yu and G. R. Brown*

Department of Chemistry, McGill University, 801 Sherbrooke Street West, Montréal, Québec, Canada H3A 2K6

Received June 9, 1992; Revised Manuscript Received August 26, 1992

ABSTRACT: The kinetics of the functionalization of poly(methyl acrylate) by reaction with ethanolamine, in dimethyl sulfoxide (DMSO) or in the binary solvents of DMSO/*o*-dichlorobenzene (DCB), to form poly(*N*-2-ethanolacrylamide) have been studied at various temperatures by means of in situ carbon-13 NMR. The data show deviation from second-order kinetics but can be fitted well by the neighboring-group model, which is characterized by three rate constants, k_0, k_1, and k_2, for reaction at sites that have no, one, or two previously reacted neighbors. In pure DMSO the reaction shows a slight retardation effect with K ($=k_1/k_0$) = 0.93 and L ($=k_2/k_0$) = 0.85. However for reaction in a 1:1 DMSO/DCB (w/w) solvent autoacceleration is observed with K = 2.0 and L = 4.0, that is independent of temperature within the experimental error. With further increase in the DCB content of the solvent, the enhancement of the reaction rate is so large that the data can no longer be fitted with the neighboring-group model. These results are consistent with preferential solvation of the copolymer coils by ethanolamine. The sequence distributions of the acrylate-centered triads of the functionalized copolymer are in good agreement with predicted values and indicate random replacement for reactions in pure DMSO and a rather blocky substitution in DCB-rich solvents.

Introduction

The preparation of poly(acrylamide) or poly(acrylate-*co*-acrylamide), of various composition, can be achieved easily by controlled functionalization of the corresponding poly(acrylate), P-COOR, by the reaction with amines, $R'NH_2$, according to

$$\text{P-COOR} + R'NH_2 \rightarrow \text{P-CONHR}' + \text{ROH} \quad (1)$$

The structure of the resulting copolymer may be tailored, to a considerable degree, by varying the structure of the polyacrylate and/or the corresponding amine.[1] In this laboratory, polymeric sorbents for bilirubin were prepared by this technique so as to obtain sorbents with systematically varied degrees of hydrophobicity.[2] The microstructure of any given functionalized polymer is, of course, controlled by the mechanism of the synthesis reaction. Hence, an understanding of the kinetics and mechanism of this reaction is crucial to the prediction of the properties of the functionalized polymers that are formed.

In spite of the utility that this reaction has in the preparation of polyacrylamide copolymers, limited information is available about its kinetics and mechanism. Undoubtedly, this reflects, at least in part, the difficulties encountered in the use of conventional analytical methods for following the functionalization and for obtaining information about the microstructure of the copolymer formed. The determination of the composition and sequence distributions of polymers is now readily accomplished by carbon-13 NMR spectroscopy.[3-6]

It has been well documented that the proximity of reacting sites can assume importance in polymer modification reactions such as reaction 1.[7-13] Evidence for the neighboring-group effect was reported by Fuoss et al.,[10] who found that the quaternization of poly(4-vinylpyridine) by reaction with *n*-butyl bromide in sulfolane departed from simple overall second-order kinetic behavior. Although a general kinetic expression was not given, the decrease in the reactivity of a pyridyl group was attributed to the presence of a quaternized neighboring group. The reaction kinetics of the chain molecules, such as vinyl polymers where each monomer residue carries a reactive substituent, exhibits a complex pattern which requires at least three rate constants, k_0, k_1, and k_2 to characterize the reactivity of residues with 0–2 reacted neighboring sites, respectively. The theoretical analysis of the kinetics was first developed by Keller[14] and has been thoroughly discussed.[8,9]

Klesper et al.[11] demonstrated, in a study of the solvolysis of syndiotactic poly(methyl methacrylate), that the monomer sequence distribution can be varied, for a given degree of conversion, by the choice of reaction conditions. Halverson and co-workers[15,16] also found that because of the neighboring-group effect, the hydrolysis of polyacrylamide in mild alkaline solution tends to produce copolymer with well-spaced ionic sites, whereas the hydrolysis in strongly acidic solution tends to develop blocks of anionic sites along the polymer chain. They suggested that copolymers of controlled microstructure can be obtained by appropriate choice of reaction conditions. Although Sawant and Morawetz[17] have proposed an experimental method by which the relative reactivity ratios K ($=k_1/k_0$) and L ($=k_2/k_0$) can be determined independently, the general way to obtain them has been to fit the data with the theoretical formulations.

In this paper we report a study of the kinetics of the functionalization of poly(methyl acrylate) (PMA) by the reaction with ethanolamine (EA) in dimethyl sulfoxide (DMSO) and in a binary DMSO/*o*-dichlorobenzene (DCB) solvent by means of an in situ ^{13}C NMR technique. The present investigation provides a relatively direct, quantitative measurement of the kinetics of the reaction. A positive deviation from the simple second-order kinetics is observed under certain solvent conditions, and the sequence distribution of acrylate-centered triads is found to be in good agreement with the theoretical predictions.

Experimental Section

Poly(methyl acrylate) (M_w = 35 000; M_n = 10 800) was purchased from Aldrich as a 25% solution in toluene. The solvent was removed by heating in vacuo for at least 1 week at 70 °C. Ethanolamine (BDH, purity >99%) was dried with KOH pellets and used without further treatment. The reaction solutions were generally 7–8% (w/w) in DMSO-d_6 (MSD, 98%) or a DMSO-d_6/DCB-d_4 (MSD) mixture. The initial concentrations of both

* To whom correspondence should be addressed.

0024-9297/92/2225-6658$03.00/0

Table I
Kinetic Parameters for the Functionalization of PMA with EA in 1:1 DMSO/DCB (w/w) at Various Temperatures

	mol·L^{-1}		L·mol^{-1}·min^{-1}				
temp, K	$[PMA]_0$	$[EA]_0$	$10^3 k_0$	$10^3 k_1$	$10^3 k_2$	K	L
373	0.832	1.66	0.75	1.46	3.2	1.95	4.2
383	0.929	1.86	1.12	2.18	4.5	1.80	3.8
393	0.892	1.78	1.56	3.28	7.0	1.56	4.5
404	0.832	1.66	2.10	3.78	8.0	1.80	3.8

Table II
Kinetic Parameters of the Functionalization of PMA with EA at 383 K in Solvents with Various Ratios of DMSO/DCB

DMSO/	mol·L^{-1}		L·mol^{-1}·min^{-1}				
DCB	$[PMA]_0$	$[EA]_0$	$10^3 k_0$	$10^3 k_1$	$10^3 k_2$	K	L
N/A	0.81	1.62	1.78	1.66	1.5	0.93	0.85
2:1	0.90	1.80	1.56	1.56	1.6	1.0	1.0
1:1	0.93	1.86	1.12	2.02	4.3	1.80	3.8
1:2.5	0.98	1.97	1.01	1.90	3.9	1.89	3.9
1:4	1.14	2.29	1.01	1.74	3.6	1.72	3.6

PMA and EA as well as the compositions of the binary solvents are given in Tables I and II.

Carbon-13 NMR spectra were obtained at 75.43 MHz with a Varian XL-300 NMR spectrometer using a variable-temperature probe. The polymer solution, contained in a 10-mm NMR tube, was preheated to the desired temperature before the EA was added. Zero reaction time was taken as the moment at which the EA was added to the polymer solution. The pulse widths were in the range 30–45°, and acquisition times were 0.91 s without a pulse delay between pulses. Because of the low signal/noise ratio, gated-decoupling procedures, which require a long pulse delay, were not used. The chemical shifts were established by referencing to DMSO at 39.5 ppm and the line intensities were obtained by integration through the Varian accessory software. The kinetics was followed by collecting sets of spectra (≥12) over a 12–18-h period.

An essentially empirical method[18,19] was used to obtain the correction factor that was needed to convert the NMR intensities into extents of reaction (ξ). It is based on the assumption that the T_1 and NOE factors are invariant with changes in the extent of reaction since the NMR measurements were all done in situ and *all* of the NMR conditions were kept identical. On this basis, the integrated intensities of the OCH_3 peaks were normalized with respect to the integrated intensities of the DMSO peaks to yield a relative intensity for the methoxy peaks, i.e., I_{OCH_3}/I_{DMSO}. These data were used to obtain a correction factor, $(I_{OCH_3}/I_{DMSO})_{t=0}$, by extrapolating the plot of I_{OCH_3}/I_{DMSO} as a function of time to $t = 0$. The reduced intensities were then converted into the extents of reaction, ξ, by

$$\xi = (I_{OCH_3}/I_{DMSO})/(I_{OCH_3}/I_{DMSO})_{t=0} \quad (2)$$

To test the validity of the assumptions, the longitudinal relaxation times (T_1) were measured, in selected experiments, by the standard inversion recovery method utilizing a 180°–τ–90° pulse sequence with a $5T_1$ pulse delay, and nuclear Overhauser enhancement effect (NOE) factors were determined with the gated decoupling pulse sequence.[20] For the methoxy carbon, T_1 (0.89 s) was found to be independent of the extent of the reaction. Attempts to derive NOE factors for the methoxy group at high reaction extent were unsuccessful due to scatter in the data resulting from the diminished intensity. For DMSO-d_6 the NOE factor remained constant, at 1.4, but a small change was detected in T_1, from an initial value of 43.2 to 44.8 s after complete reaction. The maximum uncertainty in the extent of reaction that results from this change was estimated to be <2%, as determined by use of[21]

$$M(\tau)/M_0 = (1 - E)(\sin\theta)/(1 - E\cos\theta) \quad (3)$$

where M is the magnetization and $E = \exp(-\tau/T_1)$.

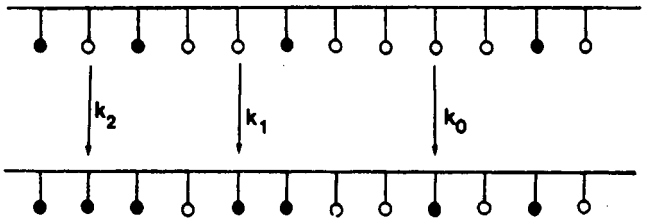

Figure 1. Kinetic scheme for functionalization of PMA with ethanolamine where the subscript i (i = 0, 1 or 2) on the rate constants indicates the number of previously reacted nearest-neighbor sites: (○) ester groups; (●) amide groups.

Results

(1) Theoretical Consideration. Theoretical analysis of the kinetics and the statistics of the chemical transformation of the functional groups on long-chain molecules was first reported by Keller[14] and have been thoroughly discussed.[8,9] In general, the process can be characterized by the reactions of functional groups having either 0, 1, or 2 previously reacted neighboring sites, respectively, characterized by the rate constants, k_0, k_1, and k_2. A schemetic description of the primary rate constants for attack of an EA molecule at a polymer ester carbonyl group, having 0, 1, or 2 nearest-neighbor amide carbonyl group(s), is given in Figure 1. The carbonyl groups along the polymer chain are represented by circles, where the open circles denote unreacted groups and the filled the reacted ones. The probability that an ester group will react in the time interval t to dt is $k_0\,dt$, $k_1\,dt$, or $k_2\,dt$, depending upon whether none, one, or two neighboring groups have already reacted at time t.

As demonstrated by Boucher,[22] for macromolecules (strictly for DP → ∞) the extent of reaction ξ, is given by

$$\xi = 1 - 2K\alpha^L\int_\alpha^1 (1-u)^2 u^{2K-L-1}\exp[-2(1-K)(1-u)]\,du - 2\alpha^L\int_\alpha^1 (1-u)u^{2K-L}\exp[-2(1-K)(1-u)]\,du - (2-\alpha)\alpha^{2K}\exp[-2(1-K)(1-\alpha)] \quad (4)$$

where the neighboring group effect is reflected by

$$K = k_1/k_0 \qquad L = k_2/k_0 \quad (5)$$

In eq 4, α is a time variable that, for the bimolecular functionalization reaction, is given by

$$\alpha = \exp[-\int_0^t k_0 C_{EA}^\circ (C_{EA}/C_{EA}^\circ)\,dt] \quad (6)$$

where C_{EA}° and C_{EA} are the initial and instantaneous concentrations of ethanolamine, respectively. Thus, in the present reaction eq 6 accounts for the depletion of the reagent as the reaction proceeds. To obtain α, the quantity C_{EA}/C_{EA}° was integrated over suitable time intervals, using the value of k_0 obtained separately from second-order plots in the limit $t \to 0$. In principle, the integrations may be carried out either analytically or numerically. In the present study, the numerical integrations were carried out by computer.

An overall second-order bimolecular reaction corresponds to $K = L = 1$ or $k_0 = k_1 = k_2$ for which the data can be plotted according to the conventional form

$$F(t) \equiv \frac{1}{C_{EA}^\circ - C_{MA}^\circ}\ln\frac{C_{MA}^\circ(C_{EA}^\circ - x)}{C_{EA}^\circ(C_{MA}^\circ - x)} = k_0 t \quad (7)$$

or

$$F'(t) = \ln\frac{1 - (C_{MA}^\circ/C_{EA}^\circ)\xi}{1 - \xi} = k_0(C_{EA}^\circ - C_{MA}^\circ)t \quad (8)$$

where C_{MA}° is the initial concentration of repeat units of

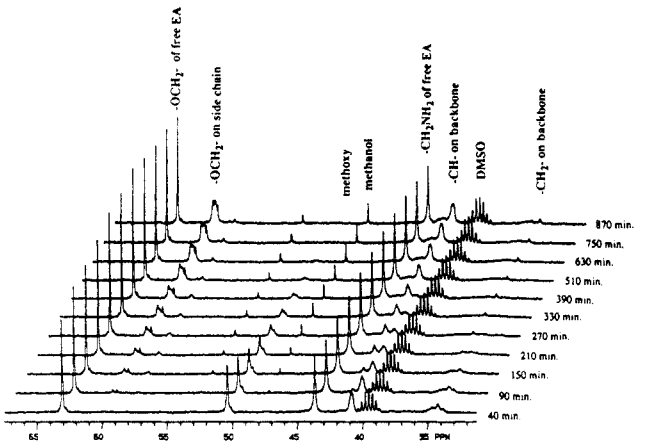

Figure 2. Stack plot of typical ^{13}C NMR spectra, showing the dependence of the intensities of the methoxy resonance on the reaction time (404 K, DMSO/DCB = 1:1).

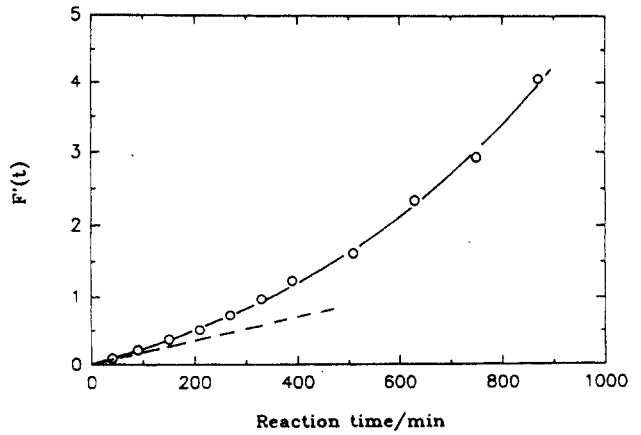

Figure 3. Conventional second-order kinetic plot of $F'(t)$ as a function of time of reaction of PMA with EA in DMSO/DCB (1:1) at 130 °C. The tangent to the curve at $t = 0$ (dashed line) gives $k_0 = 2.10 \times 10^{-3}$ L·mol^{-1}·min^{-1}.

PMA and, as defined above, ξ is the extent of reaction. Deviations from linearity can result when previously reacted sites retard subsequent reaction, evidenced by curvature toward the time axis, or when there is acceleration that results in curvature toward the $F'(t)$ axis.

Having obtained a suitable range of values of α for a particular reaction, the next step in comparing theory with experimental data was to evaluate ξ, from eq 4, for several pairs of K and L values by use of the simple "simplex" rules.[23] To do this, the theoretical plots of ξ as a function of t were superimposed on the corresponding plots of ξ_{obs} as a function of t_{obs}. The quality of the fit was tested by evaluating the deviations of the experimental points from the theoretical plots.

(2) Functionalization in 1:1 DMSO/DCB Solutions at Various Temperatures. A typical set of NMR spectra, given in Figure 2, show the progress of the reaction of PMA with EA in 1:1 DMSO/DCB (w/w) solvent. As shown in Figure 3, for a typical reaction at 110 °C the second-order plot of $F'(t)$ as a function of time, based on eq 8, clearly deviates from linearity with upward curvature; i.e., it is a reaction with autoacceleration. From this plot the rate constant k_0 (Table I) can be derived using the slope of the tangent to the curve in the limit as $t \rightarrow 0$. The solid line in Figure 4 represents the best fit to the experimentally determined values (open circles) of the extent of reaction (ξ), at various reaction times, that was obtained by use of the derived value of k_0 ($=1.12 \times 10^{-3}$ L·mol^{-1}·min^{-1}) in the neighboring-group model, eq 4, with $K = 1.80$ and $L = 3.8$.

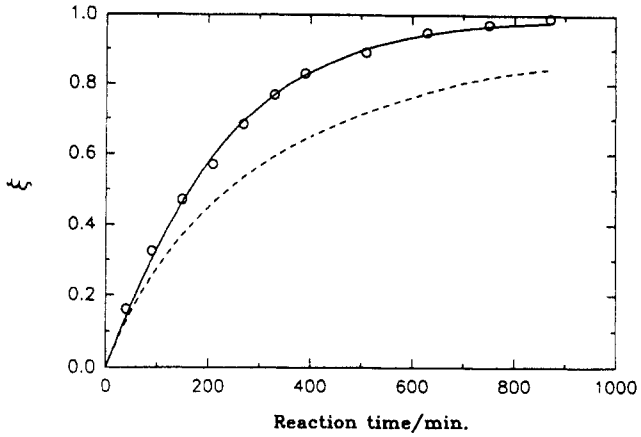

Figure 4. Typical plot of the extent of reaction, ξ, as a function of reaction time. The solid line shows the best fit to the experimental data (○) by use of the neighboring group model with $k_0 = 2.10 \times 10^{-3}$, $K = 1.80$ and $L = 3.8$. The broken line is the second-order curve, i.e., $K = L = 1$.

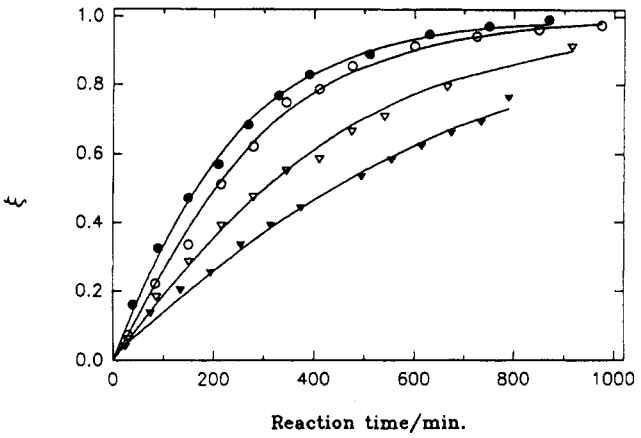

Figure 5. Dependence of extent of reaction, ξ, on reaction time at various temperatures: (●) 404 K; (○) 393 K; (▽) 383 K; (▼) 373 K. The solid lines represent the fit to the data by the neighboring group model.

The dashed line gives the time dependence of ξ for a simple second-order reaction ($K = 1$; $L = 1$) for comparison.

The importance of the neighboring group effect on the time dependence of the extent of reaction, ξ, for the functionalization of PMA with EA in a DMSO/DCB (1:1) solution is shown in Figure 5. The curves showing the best fit to the data were obtained from the theoretical analysis as summarized above. The derived rate constants and values of K and L are given in Table I. The goodness of fit, calculated from the deviations between the filled curve and experimental values of ξ, gave standard deviations σ that were always <2%.

Arrhenius plots (Figure 6), based on the assumption that there are three activation energies, $E_{a,0}$, $E_{a,1}$, and $E_{a,2}$, corresponding to k_0, k_1, and k_2, respectively, gave $E_{a,0} = 41$, $E_{a,1} = 39$, and $E_{a,2} = 38$ kJ·mol^{-1}, respectively, and may be taken as identical within the experimental error so that K and L are also temperature independent.

(3) Functionalization in Solvents with DMSO/DCB Ratios. The change of the DMSO/DCB ratio of the solvent for the functionalization of PMA with EA at 110 °C has a dramatic influence on the values of k_0, K, and L (Table II). For the reaction in pure DMSO, both K and L are slightly less than 1 so that the conventional overall second-order plot curves downward toward the time axis. For the reaction in 2:1 DMSO/DCB solvent, a linear second-order plot was obtained with a correlation factor $r = 0.996$. An abrupt increase in both K and L, of comparable magnitude,

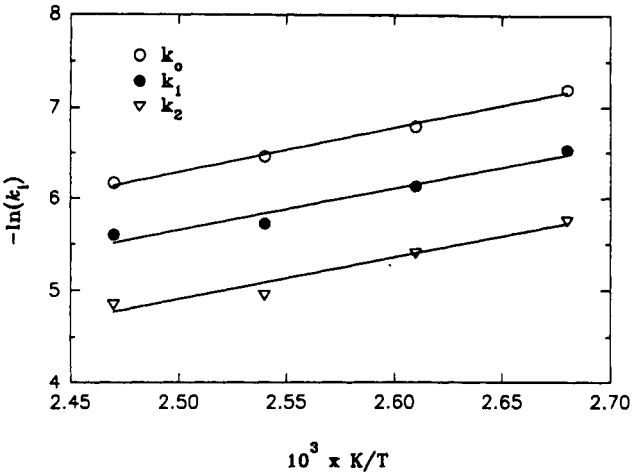

Figure 6. Arrhenius plots for the functionalization of PMA with EA in 1:1 DMSO/DCB (w/w), where $i = 0$–2 indicates the number of previously reacted nearest neighbor sites.

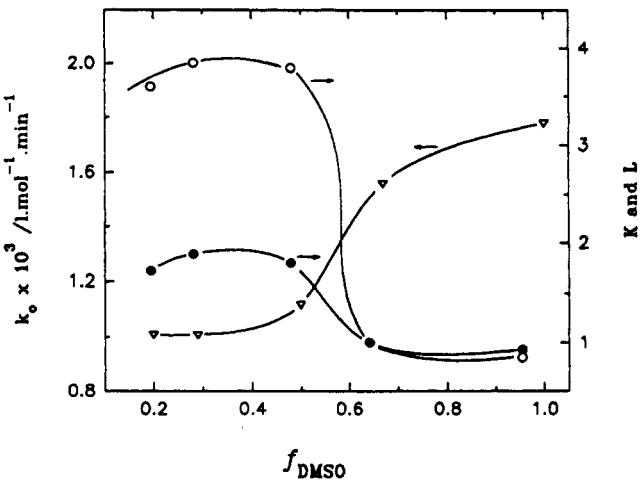

Figure 7. Dependence of k_0 (▽), K (●), and L (○) on the weight fraction (f_{DMSO}) of DMSO in the solvent.

occurred as the DMSO content of the solvent was decreased to less than 60 wt/wt % (Figure 7). Simultaneously, k_0 increased by more than 60%. For the reactions in solvents with lower DMSO content, e.g., the reaction in 1:1 DMSO/DCB solvent, an acceleration in rate was observed with increase in the extent of reaction yielding $K = 1.80$ and $L = 3.8$. Because EA does not dissolve in pure *o*-DCB, although PMA does, no data are available for the functionalization in the pure *o*-DCB.

For the reactions in DMSO/DCB (w/w) solvents having the ratios 1:2.5 and 1:4, respectively, phase separation occurred upon cooling when the reactions were complete. Concomitantly, the data deviated strongly from the theoretical model, to the point that the neighboring-group model could no longer fit the data for $\xi > 62\%$. Typical data are shown in Figure 8, where the open circles represent the experimental points and the solid line represents the theoretical values together with two dashed lines representing the cases for $K = 5$, $L = 10$ and $K = 1$, $L = 1$, respectively, for the sake of comparison. Furthermore, two new peaks, for which the chemical shift changed with the reaction extent, ξ, developed in the NMR spectra (Figure 9). They are assigned to the two carbon atoms of ethanolamine molecules involved in the solvation of the copolymer, as described in the Discussion.

(4) Triad Sequence Distributions. The occurrence of autoacceleration, as indicated by K and L values that are greater than 1, should be reflected by a tendency toward "blockiness" in the sequence distribution of the copolymer

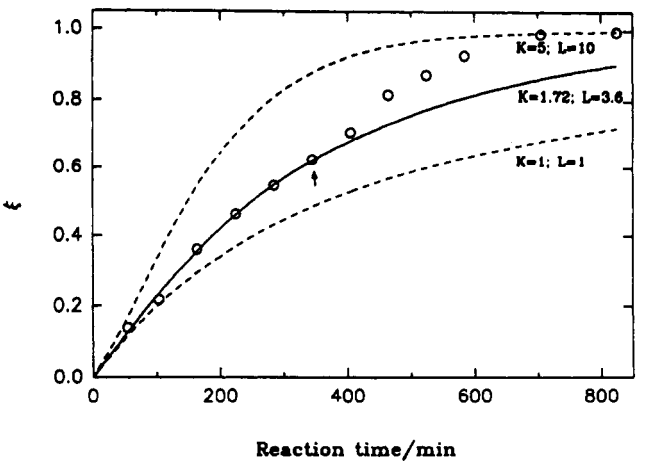

Figure 8. Dependence of the extent of reaction, ξ, on reaction time for the functionalization of PMMA with EA in DMSO/DCB (1:4) at 383 K, showing a deviation from the neighboring group model: (○) experimental value; (—) theoretical value from the neighboring group model with $K = 1.72$ and $L = 3.6$; (- - -) theoretical value with $K = 5$, $L = 10$ and $K = 1$, $L = 1$, respectively, for comparison. The arrow indicates the time at which two new peaks appear in the NMR spectra in Figure 9.

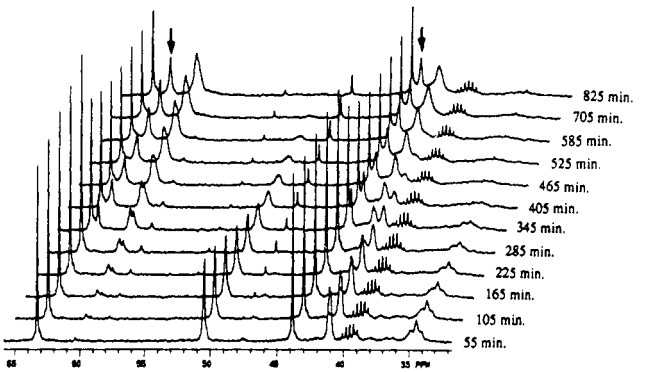

Figure 9. Stack-plot of the ^{13}C NMR spectra acquired at various reaction times for the functionalization of PMA with EA in DMSO/DCB = 1:4 (w/w). Two new peaks, indicated by the arrows, appeared in the spectra when the extent of reaction, ξ, is about 62%.

that is produced. Indeed, analyses of the sequence distribution as a function of extent of reaction permit a verification of the values of K and L.

The partially functionalized poly(methyl acrylate) can be described as a copolymer consisting of the unreacted acrylate, A, and the acrylamide, B. Thus, the three A-centered triads are AAA, AAB (=BAA), and BAB and the B-centered triads BBB, BBA (=ABB), and ABA. Due to overlap of the various methoxy (A) resonances, the derivation of the placement probabilities of the A-centered triads required a deconvolution which was achieved by computer-assuming Lorentzian line shape in the Peakfit program (Jandel Scientific Co.). Severe overlap of peaks prevented the determination of the placement probabilities of the B-centered triads.

The stack plot of the NMR spectra of the methoxy region at various reaction times in DMSO at 110 °C, shown in Figure 10a, shows that a split develops as the reaction proceeds. The deconvolution of peaks, assuming Lorentzian line shape, is illustrated in Figure 10b. The relative intensities (peak areas) were used as a measure of probabilities of the A-centered triads. The resulting sequence distributions, at various reaction times, are compared with calculated values in Figure 11, using the kinetic formulation for the neighboring group effect. The dashed lines represent the sequence distributions expected

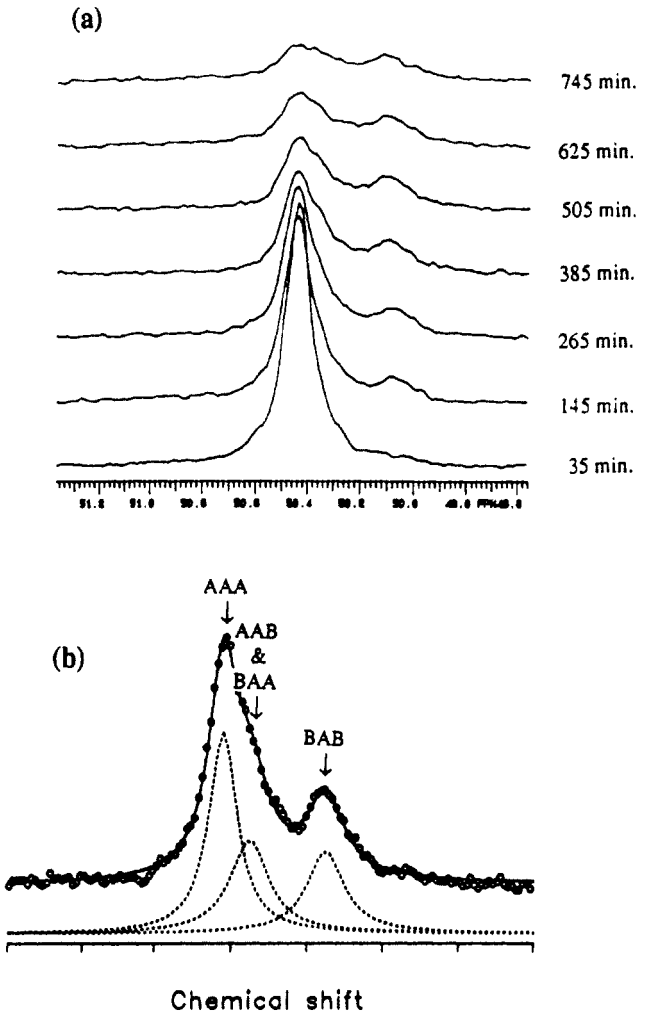

Figure 10. (a) Stack plots of ^{13}C NMR spectra for the methoxy region, taken at various reaction times (DMSO solvent at 110 °C), showing the splitting that results from the replacement of the methoxy group by the ethanolamino group. (b) Illustration of the deconvolution of the methoxy peaks of one of the above NMR spectra (reaction time = 385 min), where the points represent the experimental data, the solid line represents the fitted curve, and the dashed lines represent the theoretical peaks with Lorentzian shape. A represents the acrylate monomer, and B, the acrylamide monomer.

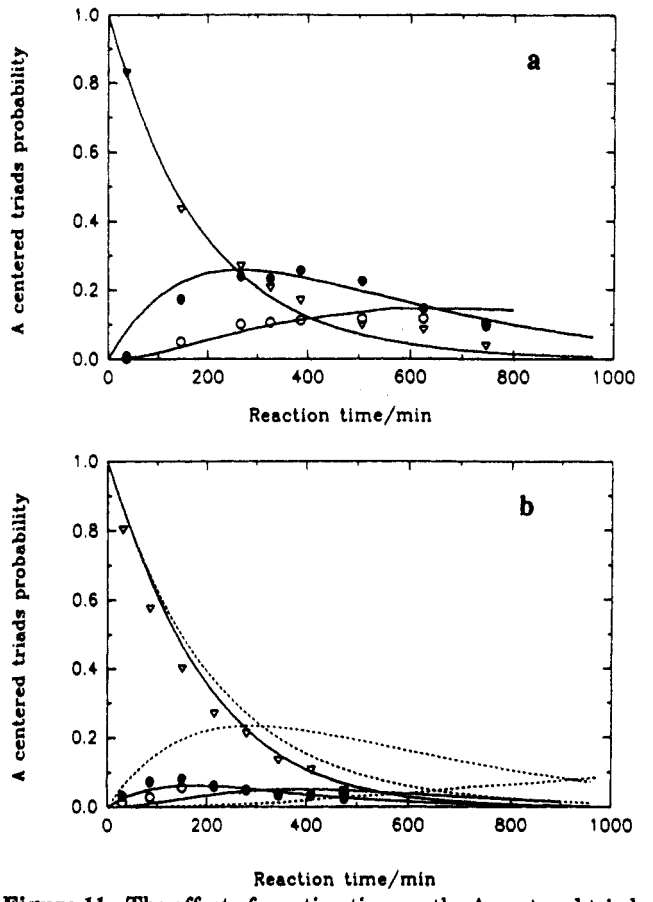

Figure 11. The effect of reaction time on the A-centered triad sequence distributions AAA (▽), AAB = BAA (●), and BAB (○). (a) Functionalization in DMSO at 110 °C. The fit to the data represents calculated values for $K = 0.93$ and $L = 0.85$. (b) Functionalization in DMSO/DCB = 1:1 (w/w). The fit to the data (solid lines) represents calculated values for $K = 2.1$ and $L = 4.5$, and the dashed lines represent the calculated values with $K = L = 1$ as a comparison.

in the absence of the neighboring-group effect, i.e., $K = 1$ and $L = 1$. Clearly, the good fit to the experimental data that is evidenced for these typical cases gives strong supporting evidence for the values of K and L derived previously by the curve fitting method.

Discussion

In addition to the usual factors that affect the kinetics of the reactions of small molecules, the rate of functionalization of PMA may be influenced by (i) the presence of previously reacted neighbors (the neighboring group effect), (ii) the tacticity of the methoxy groups on the polymer chain, and (iii) the solvent effect on the macromolecules which in solution can assume extended chain or random coil conformations with dimensions that depend on solvent composition.

By analogy with small-molecule reactions, the functionalization of PMA by reaction with EA is expected to involve a nucleophilic substitution[24] by the amine to ultimately form poly(*N*-2-ethanolacrylamide), a polymer with *N*-ethanolamide pendant groups having a terminal hydroxyl group. As expected, the rate of reaction in the aprotic polar solvent, DMSO, which stabilizes the reaction intermediate, increased as the weight fraction of DMSO (f_{DMSO}) in the binary solvent increased (Figure 7). In addition, minimal neighboring group effects are manifested because pure DMSO becomes an increasingly better solvent for the polymer as the reaction proceeds so that partially functionalized macromolecules tend to expand. The slight retardation probably reflects steric effects since the remaining methoxy groups are expected to become less accessible because of the increased size and solvation of functionalized pendant groups.

In considering the dramatic change that occurs in k_0, as well as in K and L, as the solvent polarity is decreased by addition of DCB to DMSO, it should be kept in mind that since DCB is a good solvent for PMA ($\chi = 0.59$–0.27[25]), it is likely that the PMA chains are extended in the solution at the elevated reaction temperatures. On the other hand, it is a poor solvent or, perhaps, nonsolvent for EA as well as the polar functional groups of the forming copolymer. In the less favored solvent the EA molecules have a tendency to aggregate, through polar interactions, thus lowering the effective concentration in the bulk solution and hence k_0. Theoretically, the change in the dielectric constant of the solvent can also affect k_0 by its effect on the stability of the activated complex.[26]

As a result of the polar interactions of EA with the immobilized ethanolamine at the reacted polymer sites, its effective local concentration in the vicinity of methoxy groups having either one or two previously reacted neighboring sites would be higher than in the bulk solution. Consequently, an increase in rate would be expected, with

$k_2 > k_1 > k_0$. A similar acceleration effect, reported by Kawabe and Yanagita[27] for the amination of chloromethylated polystyrene by reaction with 2-aminobutanol in dioxane, was attributed to the adsorption of 2-aminobutanol by the hydroxyl group in the nearest neighbor. This is not surprising since preferential solvation of a polymer by one of the components of a mixed solvent is a well-known phenomenon.[7]

Analysis of the data for the functionalization of PMA by reaction with EA in 1:1 DMSO/DCB solution by use of the neighboring group model shows that the values of both K and L are larger than 1, with $K \approx 2$ and $L \approx 2K$; i.e., the replacement of a methoxy group by EA accelerates the reaction rate at neighboring sites. Furthermore, since the activation energies for the reactions at these different sites are the same as that of k_0, the values of K and L are determined by the ratio of the corresponding preexponential factors.

For the reactions in DCB-rich solvent, the experimental data deviated from the theoretical neighboring group model (Figure 8). For these conditions, the kinetic data can be fit well by the neighboring group model, with K and L equal to 1.72 and 3.6, respectively, only in the region where $\xi < 62\%$. It is of interest that two new peaks appeared in the NMR spectra (Figure 9) concurrently with this deviation. In fact, a phase separation was observed upon cooling after the completion of the experiment. Preferential solvation of the polar pendent groups of the copolymer-bound EA would cause the local concentration of EA to be substantially higher than that in the bulk solution. Furthermore, it appears that the θ-condition may be approached when $\xi \geq 62\%$ so that the polymer chains tend to shrink. The local environment of the EA molecules in the domain of the polymer coils is sufficiently different from that in the bulk solution to cause a change in the chemical shift and, consequently, in the NMR spectra, so that the resonances of the two carbon atoms of these EA molecules appear as two new peaks (Figure 9).

Finally, the monomer distributions of the acrylate-centered triads are found to be in very good agreement with those that are expected from the derived values of K and L (Figure 11). On this basis it is expected that, in the functionalization of poly(methyl acrylate), copolymers of acrylate-*co*-acrylamide having the desired triad distributions can be obtained by appropriate choice of reaction conditions.

Conclusions

The kinetics and mechanism of the functionalization reaction of poly(methyl acrylate) with ethanolamine in DMSO and in the binary solvent DMSO/DCB, studied by means of in situ carbon-13 NMR at various temperatures, fit the neighboring group model. In a 1:1 DMSO/DCB solvent the functionalization reaction is autoaccelerated, with both K and L larger than 1. The acceleration effect is explained in terms of the preferential solvation of the *N*-2-ethanol pendent groups by EA molecules. The derived values of K and L are not dependent on temperature, within the experimental error. The reaction medium has an important effect on the functionalization kinetics and mechanism. For the reaction in pure DMSO solvent, at 110 °C, a slight retardation effect ($K = 0.93$ and $L = 0.85$) was found.

For the reactions in DCB-rich solvents (e.g., $f_{DCB} = 0.69$), two kinds of EA molecules were indicated in the NMR spectra when $\xi > 62\%$. The additional species is thought to be EA involved in preferential solvation of the copolymer coils. Under these conditions the enhancement of the reaction rate due to the increase in effective concentration of EA is so large that experimental data could not be fitted with the neighboring group model even though data obeyed the theoretical model well before the appearance of the evidence for preferential solvation.

These results suggest that the sequence distribution of functionalized polymers prepared by modification reactions can be controlled to a considerable degree by the appropriate choice of reaction conditions.

Acknowledgment. Financial support, in the form of operating grants, from the Natural Sciences and Engineering Council of Canada (NSERC) and the Quebec Government (Fonds FCAR) is gratefully acknowledged.

References and Notes

(1) Akelah, A.; Moet, A. *Functionalized Polymers and Their Applications*; Chapman and Hall: New York, 1990; Chapter 1.
(2) Wu, G.; Brown, G. R. *React. Polym.* **1991**, *14*, 49. St-Pierre, L. E.; Brown, G. R.; Wu, G.; Yu, Y. U.S. Pat. 5114709, 1992.
(3) Bovey, F. A. *High Resolution NMR of Macromolecules*; Academic Press: New York, 1972.
(4) Koenig, J. L. *Chemical Microstructure of Polymer Chains*; Wiley: New York, 1980.
(5) Randall, J. C. *Polymer Sequence Determination, ^{13}C NMR Method*; Academic Press: London, 1977.
(6) Zurimendi, J. A.; Guerrero, S. J.; Leon, V. *Polymer* **1984**, *25*, 1314.
(7) Morawetz, H. *Macromolecules in Solution*, 2nd ed.; Wiley: New York, 1975; Chapter 9.
(8) Boucher, E. A. *Prog. Polym. Sci.* **1978**, *6*, 63.
(9) Platé, N. A.; Noah, O. V. *Adv. Polym. Sci.* **1979**, *31*, 133.
(10) Fuoss, R. M.; Watabe, M.; Colman, B. D. *J. Polym. Sci.* **1960**, *48*, 5.
(11) Klesper, E.; Gronski, V.; Barth, V. *Makromol. Chem.* **1970**, *139*, 1.
(12) Platé, N. A. *Pure Appl. Chem.* **1976**, *46*, 49.
(13) Boucher, E. A.; Mollet, C. C. *J. Chem. Soc., Faraday Trans. 1* **1982**, *78*, 75. Boucher, E. A.; Khosravi-Babadi, E. *Ibid.* **1983**, *79*, 1951.
(14) Keller, J. B. *J. Chem. Phys.* **1962**, *37*, 2584; **1963**, *38*, 325.
(15) Panzer, H. P.; Halverson, F.; Lanster, J. E. *Polym. Mater. Sci. Eng.* **1984**, *51*, 286.
(16) Halverson, F.; Lancaster, J. E.; O'Connor, M. N. *Macromolecules* **1985**, *18*, 1139.
(17) Sawant, S.; Morawetz, H. *Macromolecules* **1984**, *17*, 2427.
(18) Shoolery, J. N.; Jankowski, W. C. Varian Application Note NMR-73-4; Varian: 1973.
(19) Blunt, J. W.; Munro, M. H. G. *Aust. J. Chem.* **1976**, *29*, 975.
(20) Freeman, R.; Hill, H. D. W.; Kaptein, R. *J. Magn. Reson.* **1972**, *7*, 327.
(21) Freeman, R.; Hill, H. D. W. *J. Magn. Reson.* **1971**, *4*, 366.
(22) Boucher, E. A. *J. Chem. Soc., Faraday Trans. 1* **1972**, *68*, 2295.
(23) Morgan, S. C.; Deming, S. N. *Anal. Chem.* **1974**, *46*, 1171.
(24) Solomons, T. W. G. *Organic Chemistry*, 2nd ed.; Wiley: New York, 1980; Chapter 17.
(25) Eguiazabal, J. I.; Fernandez-Berridi, M. J.; Iruin, J. J.; Elorza, J. M. *Polym. Bull.* **1985**, *13*, 463.
(26) Frost, A. A.; Pearson, R. G. *Kinetics and Mechanism*, 2nd ed.; Wiley: New York, 1961; Chapter 7.
(27) Kawabe, H.; Yanagita, M. *Bull. Chem. Soc. Jpn.* **1971**, *44*, 896.

Registry No. PMA, 9003-21-8; $H_2N(CH_2)_2OH$, 141-43-5.